

## Micromachined three-dimensional tunable Fabry-Perot etalons

L. Y. Lin, J. L. Shen, S. S. Lee, and M. C. Wu

UCLA, Electrical Engineering Department  
405 Hilgard Avenue, Los Angeles, CA 90095-1594

### ABSTRACT

We report on novel three-dimensional tunable Fabry-Perot etalons fabricated by surface micromachining technique. The Fabry-Perot etalons are tuned by rotation or translation movements. For the Fabry-Perot etalon tuned by rotational movement, the Fabry-Perot etalon is integrated with a rotational stage and the effective light path distance is adjusted by rotating the stage. The transmission peak wavelength shift  $\Delta\lambda_p$  of 32 nm has been observed for tuning angle  $\Delta\theta$  equal to  $70^\circ$ . For the Fabry-Perot etalon tuned by linear translation, two mirrors constituting the etalon are integrated with translational stages. The stage consists of a slider constrained by flanges along the two edges so that only translational movement along the optical axis is allowed. By changing the distance between two mirrors for 2.25  $\mu\text{m}$ , a transmission peak wavelength shift  $\Delta\lambda_p$  of 103 nm has been achieved. The three-dimensional Fabry-Perot etalons can be easily extended to integrate with other micro-optical elements fabricated in a similar way. Furthermore, fiber-to-fiber coupling will be easy with this three-dimensional approach. The three-dimensional tunable Fabry-Perot etalon is another successful demonstration of the *free-space micro-optical bench* (FS-MOB) technology we have proposed previously.

**Keywords:** three-dimensional tunable Fabry-Perot etalon, free-space micro-optical bench, integrated micro-optics

### 1. INTRODUCTION

Wavelength-division multiplexing (WDM) is an attractive approach to increase the bandwidth and routing capability of optical networks. Broadband tunable Fabry-Perot etalons are desired in WDM systems as wavelength demultiplexers. Various approaches have been proposed to increase the integrability of Fabry Perot etalons. For example, the FiEnd etalon filters invented at AT&T Bell Laboratories eliminate fiber pigtailed problems by forming mirrors directly on the cleaved ends of expanded-core fibers<sup>1</sup>. By employing photolithographic technique, micromachined Fabry-Perot interferometer with a corrugated silicon diaphragm support<sup>2</sup> and tunable micromachined gallium arsenide Fabry-Perot filters<sup>3</sup> have been realized. However, most of the microfabricated Fabry-Perot filters developed to date are restricted to the surface of substrate with light incident from the surface-normal direction, which makes fiber-to-fiber coupling more difficult and also decrease the integrability with other micro-optical elements.

Surface micromachining technique offers a new approach to implement three-dimensional free-space micro-optics monolithically. Previously, we have proposed a "*Free-Space Micro-Optical Bench* (FS-MOB)" technology for optoelectronic packaging and free-space integrated optics<sup>4,5</sup>. On the micro-optical bench, various three-dimensional micro-optical elements such as micro-lenses<sup>6</sup>, mirrors and

gratings<sup>7</sup> can be fabricated integrally on a single silicon chip by surface micromachining technique. The hybrid integration of the micro-optics with active optical devices such as semiconductor edge-emitting lasers and vertical cavity surface-emitting lasers (VCSEL) has also been demonstrated<sup>8,9</sup>. In this paper, we report on the first fabrication of novel three-dimensional tunable Fabry Perot etalons monolithically integrated with translational or rotational stages using FS-MOB technology. Their broadband tuning range will also be demonstrated.

## 2. FABRICATION

Figure 1 shows the schematic diagram of the tunable Fabry-Perot etalon with fiber mounts. The tuning is achieved by linear translation movement. The structures are fabricated integrally with microfabricated hinges and spring-latches<sup>10</sup> using two-layer-polysilicon surface micromachining technique. The fabrication process consists of deposition and patterning of two structural layers and two sacrificial layers. The first deposition is 2- $\mu\text{m}$ -thick of phosphosilicate glass (PSG) on Si substrate as sacrificial material, followed by the deposition and patterning of the first polysilicon (poly-1) layer as the first structural layer, which is 2  $\mu\text{m}$  thick. The translational stages are built on this layer with micro-hinges defined on it. Before the deposition of the second polysilicon layer (poly-2, 1.5  $\mu\text{m}$  thick), a layer of 0.5- $\mu\text{m}$ -thick of PSG is deposited as the second sacrificial material. The hinges staples which hold the hinge pins are defined on poly-2 and connected to the translational stage by via holes. The mirrors are defined on poly-2 with their bottom edges connected to the micro-hinges. The spring latches are also defined on this layer with their bottom fixed on the translational plates. There are two guiding flanges along the two edges of the translation plate to constrain the translation movement. The flanges are defined on poly-2 with their outer edges connected through the Si substrate by via stripes. The release of the structure layers is achieved by selectively etching PSG away in hydrofluoric acid. After PSG material is removed, the mirrors can be freely rotated out of the substrate with its bottom fixed on the translational plates by the micro-hinges. The spring-latches are pushed up when the mirrors are lifted up, and snap into the matched holes on the mirror plates and fix the mirrors with spring force of polysilicon material. The length of the spring-latches defines the angle between the mirror and the substrate coarsely, which is 90° in this case. The latching plates on both sides of the mirrors further increase the mechanical strength of the structures and precisely define the angles of mirrors<sup>4</sup>. A 450 Å-thick gold layer is evaporated on the mirrors before assembly to increase the mirror reflectivity. Figure 2 shows the SEM micrograph of an assembled Fabry-Perot etalon with fiber mounts.

Two types of tunable Fabry-Perot etalons are fabricated: a solid etalon and an etalon with two parallel mirror plates. The solid etalon is tuned by rotations, which is achieved by the on-chip rotatable stage. The fabrication of the rotational stage is similar to that of the translational stage except that, instead of building two guiding flanges along the two edges of the translational plate, a hub is defined on poly-2 in the axle position of the rotational poly-1 plate, with its center connected to the Si substrate by via holes<sup>11</sup>.

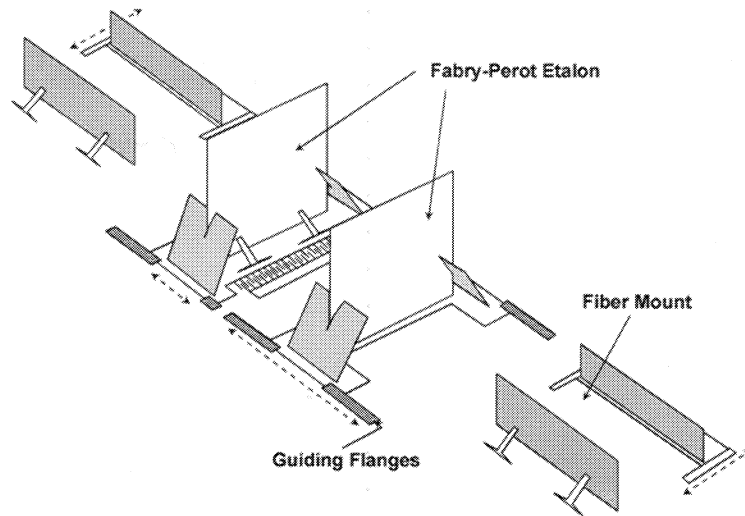


Figure 1 Schematic diagram of the micromachined three-dimensional tunable Fabry-Perot etalon.

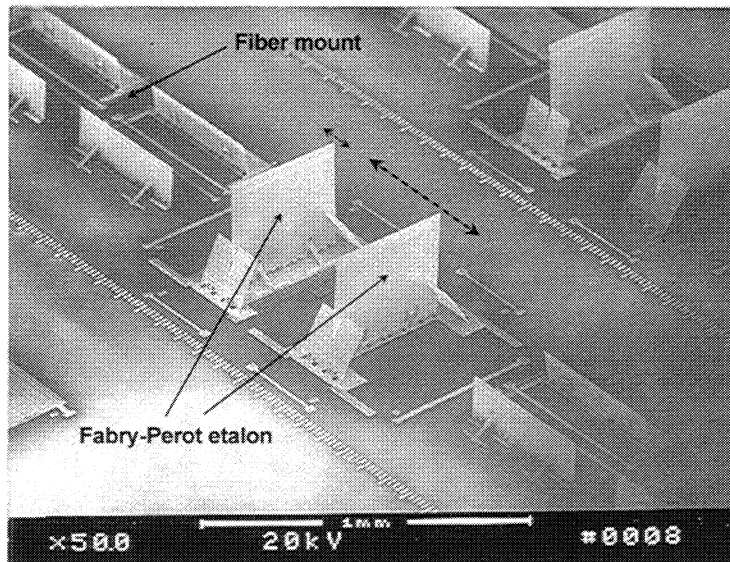


Figure 2 SEM micrograph of the assembled tunable Fabry-Perot etalon.

### 3. SOLID FABRY-PEROT ETALON

Figure 3 shows the schematic drawing of the three-dimensional solid polysilicon Fabry-Perot etalon fabricated integrally with a rotational stage, and Figure 4 is the SEM micrograph of the assembled solid Fabry-Perot etalon tuned by rotation. The transmission characteristics of the tunable etalon is analyzed using a spectrometer with white light as incident source. Figure 5 is the transmission spectrum of the solid Fabry-Perot etalon with the light source incident at normal direction. By rotating the Fabry-Perot etalon, the transmission peak wavelength changes with respect to the rotation angle according to the following relation:

$$\lambda_P = \lambda_0 \cdot \sqrt{1 - \left( \frac{\sin \theta_i}{n_{poly}} \right)^2}$$

$\theta_i$ : incident angle of the light source with respect to the normal direction of the etalon

$n_{poly}$ : refractive index of polysilicon

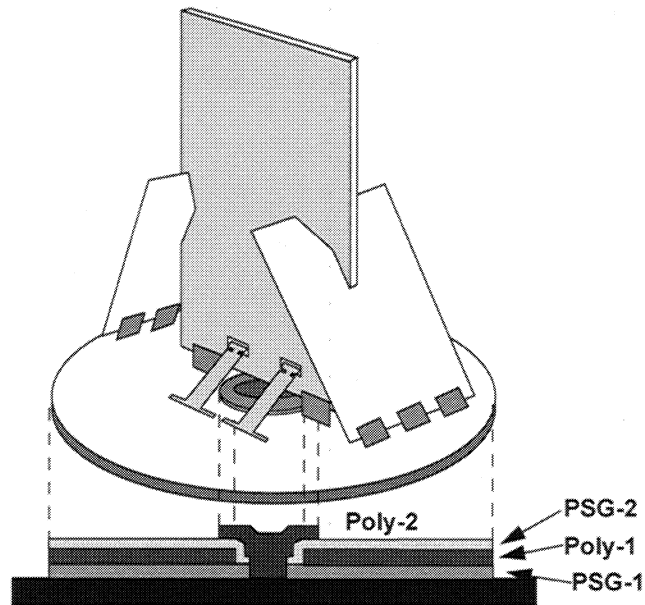


Figure 3 Schematic drawing of the solid Fabry-Perot etalon integrated with a rotational stage.

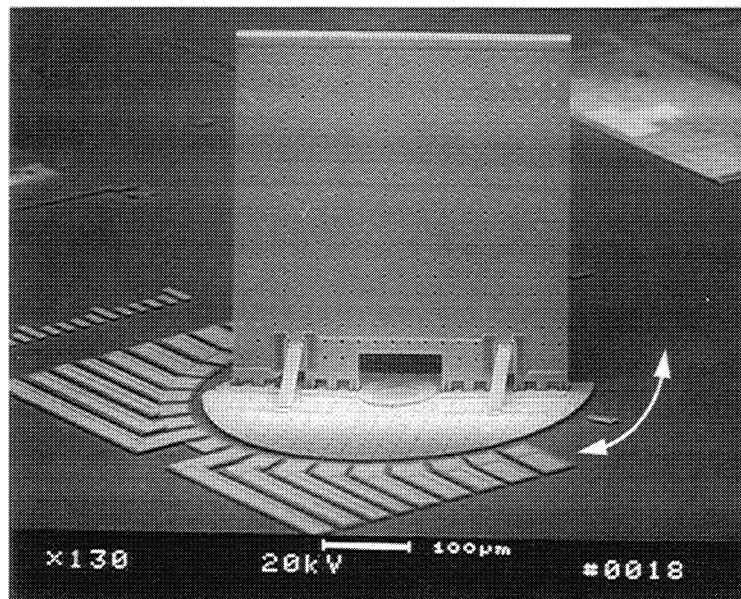


Figure 4 SEM micrograph of the assembled three-dimensional solid etalon tuned by rotation.

Figure 6 shows the result of the transmission peak wavelength tuned by rotation. The refractive index of polysilicon is 3.86 in the wavelength region of the experiment. A tuning range of 32 nm is achieved by rotating the Fabry-Perot etalon by 70°.

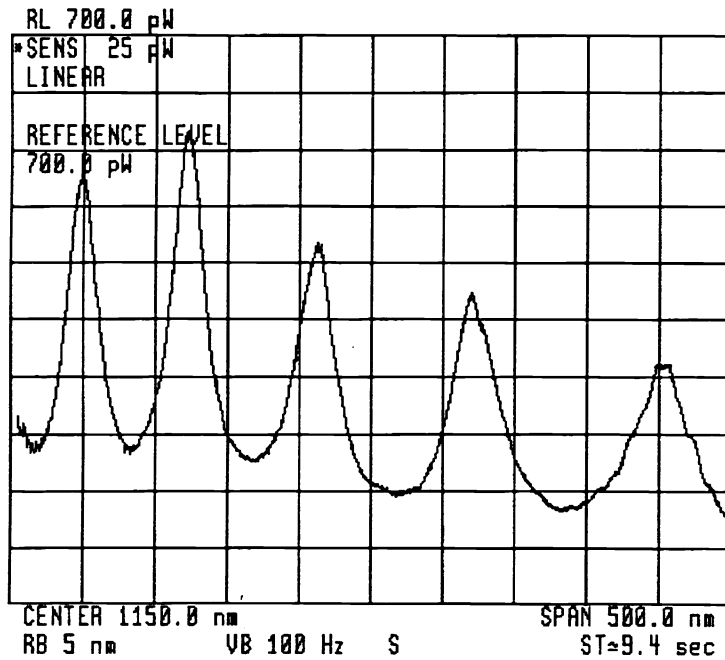


Figure 5 Transmission characteristics of the three-dimensional Fabry-Perot etalon tuned by rotation. The light source is incident normal to the etalon in this experiment.

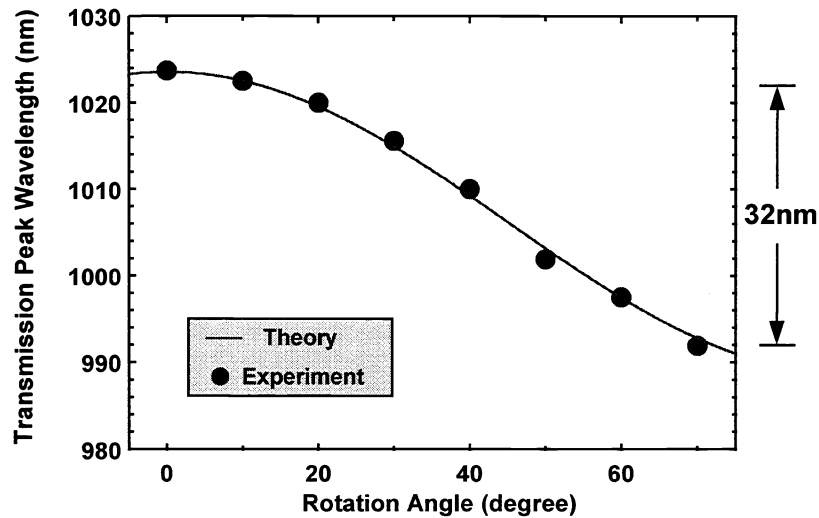


Figure 6 Transmission peak wavelength versus rotation angle of the three-dimensional Fabry-Perot etalon tuned by rotation.

#### 4 CASCADE FABRY-PEROT ETALON

The experiments of a cascade Fabry-Perot etalon is performed by testing a three-dimensional etalon similar to Figure 2, but with much shorter distance between two mirrors. The solid etalon formed by a single polysilicon plate has shorter cavity length, and therefore larger free-spectral-range (FSR). The Fabry-Perot cavity formed by two polysilicon plates (with inner sides coated by Au) has smaller FSR and smaller full-width-at-half-maximum (FWHM) for the transmission peaks. The overall effect of the cascade Fabry-Perot etalon is that larger FSR and smaller FWHM for the transmission peaks can be achieved simultaneously, therefore the finesse of the whole system can be enhanced. This is depicted in

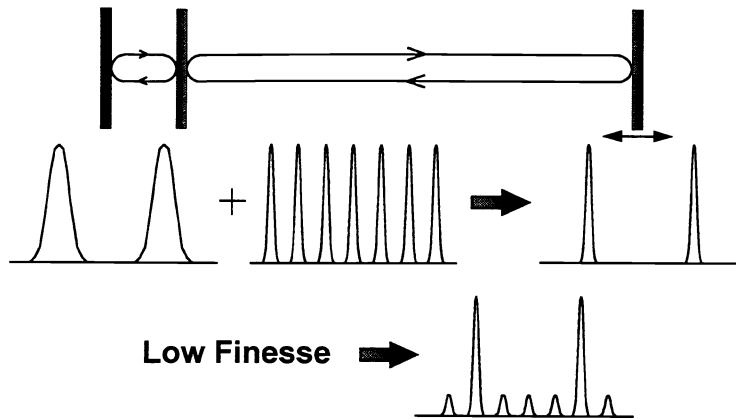


Figure 7 Overall effect of the cascade Fabry-Perot etalon.

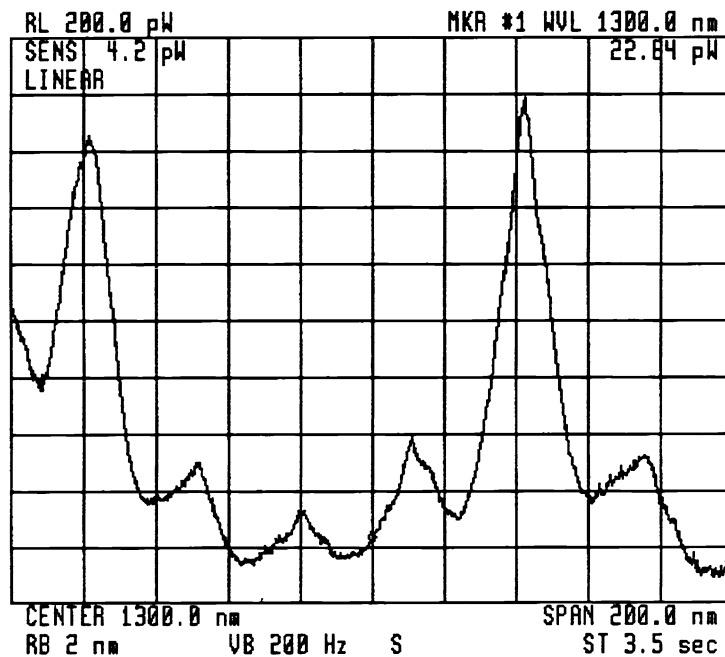


Figure 8 Transmission characteristics of the three-dimensional cascade Fabry-Perot etalon.

Figure 7. Figure 8 shows the transmission characteristic of the three-dimensional cascade Fabry-Perot etalon. As the reflectivity of the mirrors formed by Au coating is not high enough in this demonstration, there are some residue peaks in between the main peaks of the transmission spectrum. This can be improved by increasing the reflectivity of the mirrors with dielectric mirrors. The transmission peak wavelengths can be tuned by varying the distance between the two mirrors constituting the Fabry-Perot cavity. Shown in Figure 9 is the peak wavelength change versus the cavity length variation of the cascade Fabry-Perot etalon. A tuning range  $\Delta\lambda_p$  of 103 nm is achieved with cavity length change of 2.25  $\mu\text{m}$ .

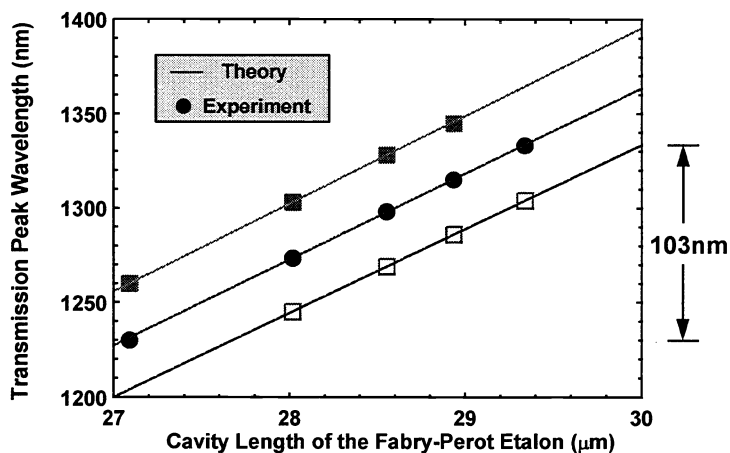


Figure 9 Transmission peak wavelength change versus cavity length of the cascade Fabry-Perot etalon.

## 5. CONCLUSION

In summary, we have demonstrated three-dimensional tunable Fabry-Perot etalons fabricated integrally with translational and rotational stages using surface micromachining technique. Tuning ranges of  $\Delta\lambda_p$  equal to 32 nm and 103 nm are achieved by rotation ( $\Delta\theta$  equal to  $70^\circ$ ) and varying the cavity length ( $\Delta d$  equal to 2.25  $\mu\text{m}$ ) of the Fabry-Perot etalon, respectively. The finesse of the system can be improved by increasing the mirror reflectivity. The three-dimensional Fabry-Perot etalons can be integrated with other free-space micro-optical elements fabricated by similar technique. This novel device has applications in wavelength-division multiplexing systems and optical sensors.

## 6. ACKNOWLEDGMENT

The authors would like to thank Professor K. S. J. Pister for valuable discussions. This project is supported in part by ARPA and Packard Foundation. Part of the devices are fabricated by the ARPA-sponsored MUMPs fabrication services.

## 7. REFERENCES

1. J. Stone, L. W. Stulz, D. Marcuse, C. A. Burrus, and J. C. Centanni, "Narrow-band FiEnd etalon filters using expanded-core fibers," *IEEE J. Lightwave Tech.*, Vol. 10, No. 12, pp. 1851-1854, 1992.
2. J. H. Jerman, D. J. Clift, and S. R. Mallinson, "A miniature Fabry-Perot interferometer with a corrugated silicon diaphragm support," *Sensors and Actuators A*, Vol. 29, pp. 151-158, 1991.
3. M. S. Wu, E. C. Vail, G. S. Li, L. Eng, and C. J. Chang-Hasnain, "Speed and polarization characteristics of widely tunable micromachined GaAs Fabry-Perot filters," *Conference on Lasers and Electro-Optics*, Paper CThL4, Baltimore, MD, May 21 ~ 26, 1995.
4. L. Y. Lin, S. S. Lee, K. S. J. Pister, and M. C. Wu, "Micro-machined three-dimensional micro-optics for integrated free-space optical system," *IEEE Photonics Tech. Lett.*, Vol. 6, No. 12, pp. 1445-1447, 1994.
5. M. C. Wu, L. Y. Lin, and S. S. Lee, "Micromachined free-space integrated optics," *Proceedings of SPIE*, Vol. 2291, *Integrated Optics and Microstructures II*, pp. 40-51, 1994.
6. L. Y. Lin, S. S. Lee, K. S. J. Pister, and M. C. Wu, "Three-dimensional micro-Fresnel optical elements fabricated by micromachining technique," *Elec. Lett.*, Vol. 30, No. 5, pp. 448-449, 1994.
7. S. S. Lee, L. Y. Lin, K. S. J. Pister, and M. C. Wu, "Three-dimensional microgratings for free-space optical interconnections and clock-distribution systems," *Conference on Lasers and Electro-Optics*, Paper CFF7, Baltimore, MD, May 21 ~ 26, 1995.
8. L. Y. Lin, S. S. Lee, K. S. J. Pister, and M. C. Wu, "Self-aligned hybrid integration of semiconductor lasers with micromachined micro-optics for optoelectronic packaging," *Appl. Phys. Lett.*, Vol. 66, No. 22, pp. 2946-2948, 1995.
9. S. S. Lee, L. Y. Lin, K. S. J. Pister, and M. C. Wu, "Passively aligned hybrid integration of  $8 \times 1$  vertical cavity surface-emitting laser arrays for free-space optical interconnect," to be published in *IEEE Photonics Tech. Lett.*, September, 1995.
10. K. S. J. Pister, M. W. Judy, S. R. Burgett, and R. S. Fearing, "Microfabricated hinges," *Sensors and Actuators A*, Vol. 33, pp. 249-256, 1992.
11. L. S. Fan, Y. C. Tai, and R. S. Muller, "IC-processed electrostatic micromotors," *Sensors and Actuators*, Vol. 20, pp. 41-47, 1989.